Mn^{II}—A fascinating oxidation catalyst: Mechanistic insight into the catalyzed oxidative degradation of organic dyes by H$_2$O$_2$

Erika Ember [a], Hanaa Asaad Gazzaz [a,b], Sabine Rothbart [a], Ralph Puchta [a,c], Rudi van Eldik [a,*]

[a] Inorganic Chemistry, Department of Chemistry and Pharmacy, University of Erlangen-Nürnberg, Egerlandstr. 1, 91058 Erlangen, Germany
[b] Department of Chemistry, King Abdul-Aziz University, Jeddah, Saudi Arabia
[c] Computer Chemistry Center, University of Erlangen-Nürnberg, Nägelsbachstr. 25, 91052 Erlangen, Germany

ARTICLE INFO

ABSTRACT

The use of simple Mn^{II} ions as efficient catalyst precursors for the oxidation of different highly stable organic dyes using H$_2$O$_2$ as an environmentally benign oxidant under mild reaction conditions, is presented. The role of a series of aromatic dyes in the in situ formation and stabilisation of the active catalyst was studied in detail using stopped-flow techniques and UV–Vis detection. DFT calculations were employed to predict the nature of the role of the substrate in the stabilisation of highly reactive Mn^{II} intermediates. Furthermore, low-temperature EPR measurements were performed in order to characterize the in situ formed catalytically active Mn^{IV}=O intermediate responsible for the fast and versatile oxidation of organic dyes in aqueous solution.

© 2009 Elsevier B.V. All rights reserved.

1. Introduction

Transition metal ions play a critical role in various oxidation and electron transfer processes in natural and industrial processes, and in academic chemistry [1]. In recent years, considerable advances have been made in the development of atom efficient and environmentally friendly catalytic methods employing H$_2$O$_2$ [2], most notably in the use of transition metal catalysts in the oxidation of different organic substrates. Among the various transition metal catalysts for oxidation, manganese stands out as one of the most efficient, economic and environmental benign element. Various manganese complexes with different salen [3], porphyrin [4], TACN (1,4,7-triazacyclononane) [5] and aromatic N-donor ligands [6] are known to be efficient catalysts for the oxidation of a wide range of organic substrates. However, often cost effectiveness and robustness are the major obstacles associated with the application of these metal complexes in industrial processes.

In an earlier study by Oakes et al. [7] on the Mn^{II} catalyzed oxidative degradation of Calmagite (3-hydroxy-4-(2-hydroxy-5-methylphenylazo)naphthalene-1-sulfonic acid), a dye containing the *o,o′*-dihydroxy azo structural motif, the potential use of Mn^{II} salts as oxidation catalyst was demonstrated for various dyes with high binding affinity using peroxosulfate as oxidizing agent in

alkaline media. However, when Calmagite was replaced by a related organic dye with lower binding capacity, no oxidation occurred [7]. Later reports by Lane et al. [8] and Ho et al. [9] on the Mn^{II} catalyzed epoxidation of different electron rich and substituted alkenes in the presence of H$_2$O$_2$ or peracetic acid in a bicarbonate containing solution, demonstrated the usability of Mn^{II} ions as effective epoxidation catalyst of alkenes.

In our recent study on the oxidative degradation of the azo dye Orange II ([4-[(2-hydroxynapthyl)azo]benzenesulfonic acid], sodium salt) by H$_2$O$_2$ catalyzed by simple Mn^{II} salts in aqueous bicarbonate containing solution under mild reaction conditions, it was possible to prove that an efficient oxidation of dye could be achieved in the presence of catalytic amounts of simple Mn^{II} ions [10]. It was also possible to demonstrate that starting from a Mn^{II} salt in bicarbonate containing solution under catalytically relevant experimental conditions, different highly reactive manganese intermediates are formed, which in the absence of any further coordinating ligands rapidly decompose with the formation of insoluble Mn(OH)$_2$, MnCO$_3$ or MnO$_2$, depending on the selected reaction conditions. An effective stabilisation of the in situ formed reactive intermediates could be achieved in the presence of an electron rich organic molecule, such as the dye itself. Subsequently, the catalytic activity of the in situ formed manganese intermediate was evaluated by performing the oxidation reaction in the presence of repeatedly added substrate and H$_2$O$_2$ without any significant loss in activity, indicating an excellent stability of the in situ formed catalyst. For this purpose, the aim of the present study

---

was to investigate the potential use of simple Mn^{II} salts as catalysts in oxidative degradation of various dyes, which due to their high solubility and stability in water represent a real environmental problem, and to check the performance of the catalytic process in a practical case. To rationalize the experimental data, a theoretical investigation based on the combined use of density functional theory (DFT) and conductor-like polarizable continuum model (CPCM) calculations has also been performed.

2. Experimental

2.1. Materials

Unless otherwise stated, all chemicals were commercially available (Acros Organics, Germany) and were used without any further purification. Hydrogen peroxide 35 wt.%, as well as different manganese salt hydrates used in the experiments, were of analytical grade and provided by Acros Organics (Germany). Carbonate buffer solutions were prepared using sodium bicarbonate (Acros Organics, Germany) in deionised water at ambient temperature.

2.2. Equipment

Kinetic measurements were performed in a reaction vessel using a Hellma 661.502-QX quartz Suprasil immersion probe attached via optical cables to a 150 W Xe lamp and a multi-wavelength J&M detector, which records complete absorption spectra at constant time intervals. UV–Vis spectra were recorded on a Shimdazu UV-2101 spectrophotometer at 25 °C. The pH of the buffer solution was carefully measured using a Mettler Delta 350 pH meter previously calibrated with standard buffer solutions at two different pH values (4 and 10).

2.3. General procedure

Oxidation reactions were performed in a laboratory scale bath reactor equipped with a magnetic stirrer. 2×10^{-5} M catalyst solution and 0.01 M H_2O_2 (required due to the undesired catalase activity of Mn^{II}) were added to 40 ml of 5×10^{-5} M dye (limited by the high extinction coefficients of the dyes) at a pH ranging from 8 to 10 at 25 °C. In all the experiments the concentration of H_2O_2 was high enough not to constitute a limiting factor for effectiveness of the system. First order rate constants, where possible, were calculated using Specfit/32 and Origin (version 7.5) software. To estimate the effect of the catalyst and H_2O_2 concentrations on the catalytic reaction at different carbonate concentrations, kinetic measurements were carried out using an SX.18MV stopped-flow instrument from Applied Photophysics.

2.4. Spectrophotometric titration

A 0.88 cm path length tandem cuvette with two separate compartments (0.44 cm path length each), was filled with 1 ml 5×10^{-5} M organic dye stock solution in one, and different concentrations of an aqueous $Mn(NO_3)_2$ solution in the other compartment. The cuvette was placed in the thermostated cell holder of the spectrophotometer for 10 min. UV–Vis spectra were recorded before and after mixing the solutions. The resulting spectra present the sum of the two individual spectra before, and that of the reaction mixture, after mixing. The observed spectral change is a result of complex-formation between Mn(II) and the organic dye.

2.5. EPR measurements

Perpendicular mode EPR spectra were recorded on an X-band Joel Jes Fa 200 spectrometer equipped with a cylindrical mode cavity and a liquid helium cryostat. The EPR measurements were performed in quartz tubes at 7 K. Data analyses were done with the Jes-Fa Series software package.

2.5.1. Sample preparation

The Mn^{II}-bicarbonate was prepared by mixing a solution of 2×10^{-4} M $Mn(NO_3)_2$ with 0.4 M $NaHCO_3$ at pH 8.5. In a similar way the catalytically active $Mn^{IV}=O$ intermediate was prepared starting from a 2×10^{-4} M $Mn(NO_3)_2$ and 10^{-2} M H_2O_2 in a 0.4 M $NaHCO_3$ containing aqueous solution at pH 8.5. The in situ formed reactive Mn intermediates are stable for several minutes at ambient temperature, after which a white brownish precipitate of $MnCO_3$ and MnO_2 is formed, respectively. Therefore, immediately after its formation, EPR quartz tubes were rapidly filled and the solution was frozen by immersing the samples into liquid nitrogen before precipitation took place. The samples were mounted afterwards into the EPR probehead that was placed into the precooled cryostat at 7 K. In addition, the formation of different reactive Mn intermediates was studied under catalytically relevant experimental conditions at 7 K.

2.6. DFT calculations

Unrestricted B3LYP/LANL2DZ hybrid density functional calculations [11a–c], i.e. with pseudo-potentials on the heavy elements and the valence basis set [11d–f] augmented with polarization functions (further denoted as B3LYP/LANL2DZp) [11g] were carried out using the Gaussian 03 [12] suite of programs. The relative energies were corrected for zero point vibrational energies (ZPE). The resulting structures were characterized as minima by computation of vibrational frequencies, and the wave functions were tested for stability. The performance of the computational level employed in this study is well documented [10,13]. Further energy computations were carried out using the conductor-like polarizable continuum model (CPCM) [14].

3. Results and discussion

3.1. Role of substrate in the formation and stabilisation of in situ formed reactive intermediates in aqueous solution

The rational design and fine-tuning of catalysts to attain sufficient stability, reactivity and selectivity for various oxidation reactions, represents a major difficulty in the elaboration of new and powerful technologies. The substrate scope represents one of the critical factors for the development of efficient and most of all environmentally safe oxidative degradation systems [15]. Thus, a key aspect for an ideal oxidative degradation method is its applicability for a large number of different substrates. In order to understand the role played by different organic dyes (see Fig. 1) acting as mono- or bidentate ligands in the stabilisation of the in situ formed catalyst, the oxidative degradation of various dyes was studied using catalytic amounts of Mn^{II} salt and a green oxidizing agent, e.g. H_2O_2, under mild reaction conditions. Table 1 lists the characteristic absorption bands, pK_a values and the observed first order rate constant determined under the experimental conditions quoted.

3.1.1. Oxidative degradation of aromatic azo dyes (AY, MO and PADA)

The oxidative degradation of aromatic azo dyes acting as a monodentate ligand, i.e. AY, MO and PADA, were performed in the presence of catalytic amounts of Mn^{2+} and 0.01 M H_2O_2 at pH 8.5 in a bicarbonate containing buffer solution. The UV–Vis absorbance-time traces of the reaction course for the studied dyes are shown in Fig. 2.
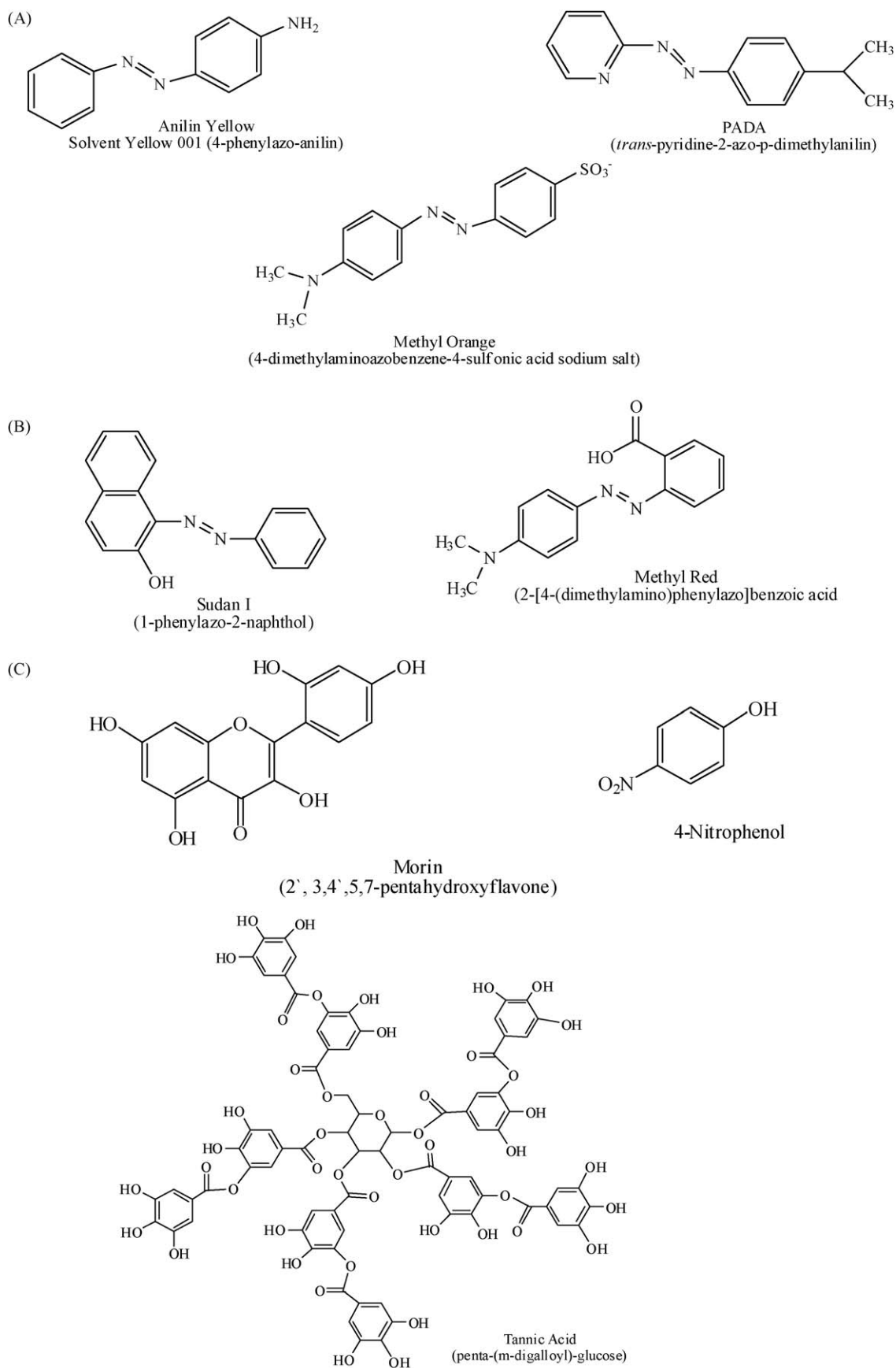
(A)

Anilin Yellow
Solvent Yellow 001 (4-phenylazo-anilin)

PADA
(*trans*-pyridine-2-azo-p-dimethylanilin)

Methyl Orange
(4-dimethylaminoazobenzene-4-sulfonic acid sodium salt)

(B)

Sudan I
(1-phenylazo-2-naphthol)

Methyl Red
(2-[4-(dimethylamino)phenylazo]benzoic acid)

(C)

Morin
(2`, 3,4`,5,7-pentahydroxyflavone)

4-Nitrophenol

Tannic Acid
(penta-(m-digalloyl)-glucose)

Fig. 1. Structural formulae for the dyes used in this study: (A) aromatic azo dyes without functional group attached to the azo linkage, (B) aromatic azo dyes with functional groups adjacent to the azo linkage and (C) phenolic derivatives and flavonoid dyes.

Table 1
Characteristic absorption bands, pK_a values [16] and observed rate constants k_{obs} for the oxidation of the studied organic dyes.

Studied dye	Absorption λ_{max} (nm)	pK_a [16]	k_{obs} (s^{-1})[a]
Aniline Yellow (AY)	370	2.7 [16a]	0.010 ± 0.002
PADA	460	4.5 [16b]	0.055 ± 0.004
Methyl Orange (MO)	470	3.7 [16c]	0.052 ± 0.0003
Sudan I (S I)	490	11 [16c]	0.084 ± 0.007
Orange II (O II)	480	11.4 [16c]	0.021 ± 0.001
Methyl Red (MR)	430	5.2 [16d]	0.047 ± 0.0003
4-Nitrophenol (PNP)	400	7.08 [16e]	0.025 ± 0.0005
Morin (M)	400	4.8, 7 [16f]	0.107 ± 0.003
Tannic acid (TA)	450	9.9 [16g]	0.023 ± 0.008

[a] Experimental conditions: 2×10^{-5} M Mn(NO$_3$)$_2$, 5×10^{-5} M dye, 0.01 M H$_2$O$_2$, pH 8.5, 0.4 M total carbonate and 25 °C.

As it can be observed, an effective decomposition of AY was reached using simple Mn^{II} salts as oxidation catalyst and H$_2$O$_2$ within less than 400 s under the experimental conditions mentioned above (see Fig. 2). After approximately 600 s, the precipitation of coloured reaction products in solution was observed, leading to an increase in the absorbance intensity at 370 nm (see Fig. 2 and Fig. S1A, Supporting Information).
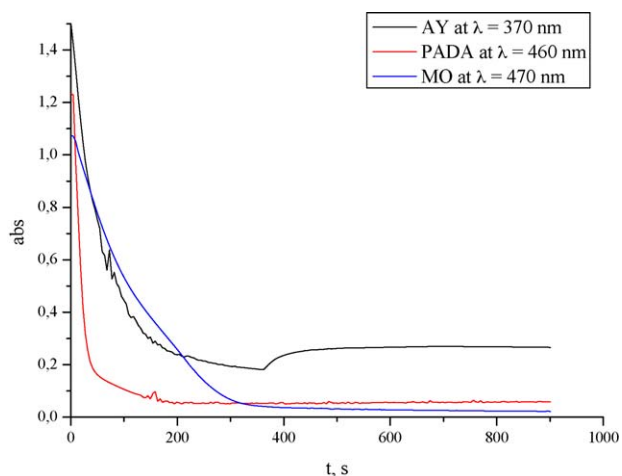

Fig. 2. Comparison of the absorbance changes observed at different characteristic wavelength for the 2×10^{-5} M Mn(NO$_3$)$_2$ catalyzed oxidative degradation of 5×10^{-5} M azo dyes in the presence of 0.01 M H$_2$O$_2$ at pH 8.5 (0.4 M HCO$_3^-$) and 25 °C.

In order to study the ability of AY to stabilize the in situ formed catalyst under the experimental conditions mentioned above, the Mn^{II} containing dye solution was allowed to stand for a few minutes at room temperature [17] before H$_2$O$_2$ was added. No difference in the reaction course was observed, when the reaction was started upon concomitant addition of the catalyst and H$_2$O$_2$ to the AY containing buffer solution or when it was previously added to the dye containing buffer solution (see Figs. S1 and S2, Supporting Information), indicating the rapid formation of stable and reactive Mn^{II} intermediates in solution.

In the case of PADA, the increased electron donating ability of the pyridinic nitrogen functionality is considered to be responsible for the rapid formation of the stable Mn–dye intermediate and the fast and efficient decomposition of the dye in the presence of H$_2$O$_2$ under catalytically relevant experimental conditions (see Fig. 2).

UV–Vis spectra of MO recorded in the presence of 2×10^{-5} M Mn^{II} and 0.01 M H$_2$O$_2$ when the catalyst was added along with the H$_2$O$_2$ to the dye, and when the catalyst was kept in the dye containing buffer solution before the addition of H$_2$O$_2$, are shown in Fig. 3.

In the case of MO, an aromatic azo dye without functional groups attached to the azo linkage, after the addition of catalyst and H$_2$O$_2$ to the dye containing buffer solution, fast decomposition of the substrate followed by the formation of N,N-dimethyl-4-nitroaniline, an intermediate oxidation product of MO oxidation [18], was observed (see also Fig. S3A, Supporting Information).

In order to study the stabilisation ability of MO in the case of the Mn^{II} catalyzed oxidation of organic dyes by H$_2$O$_2$, the dye and catalyst containing solution was allowed to stand for 20 h (sufficient time to deactivate non-coordinated Mn^{II} ions in the absence of a coordinating ligand in bicarbonate solution) at room temperature (see Fig. 3B). After the reaction was initiated by the addition of an appropriate amount of H$_2$O$_2$ to the reaction mixture, fast decomposition of the substrate along with the formation of intermediates occurred within less than 400 s (see Figs. 2 and 3B and S3B, Supporting Information). However, for a complete decomposition of the investigated substrate, higher concentrations of H$_2$O$_2$ and longer reaction time are required.

3.1.2. Oxidative degradation of aromatic azo dyes with functional groups adjacent to the azo linkage (S I and MR)

To explore the influence of aromatic substitution patterns on azo dye degradability, the oxidative degradation of *ortho* substituted azo dyes under catalytically relevant experimental conditions were studied. For the 2×10^{-5} M Mn^{2+} catalyzed
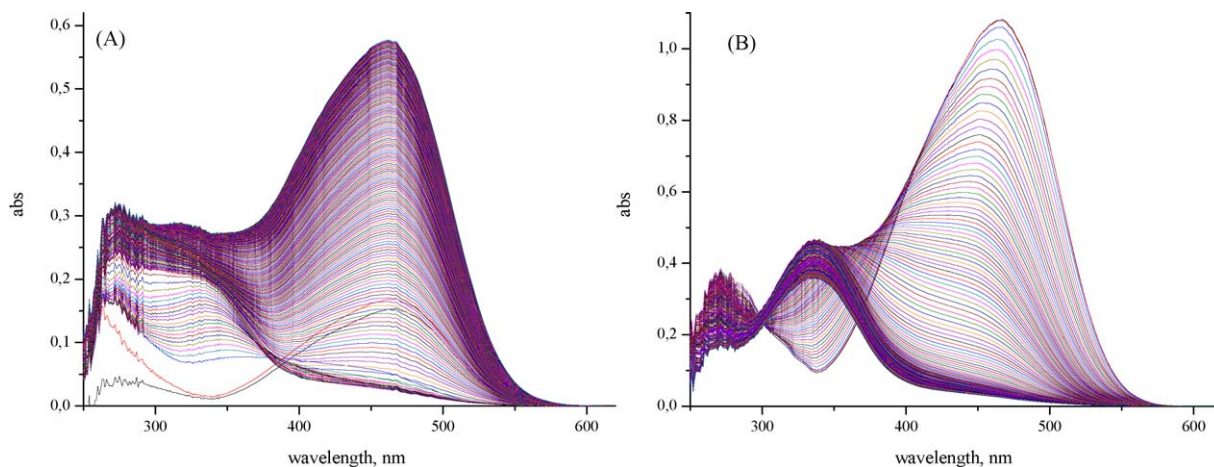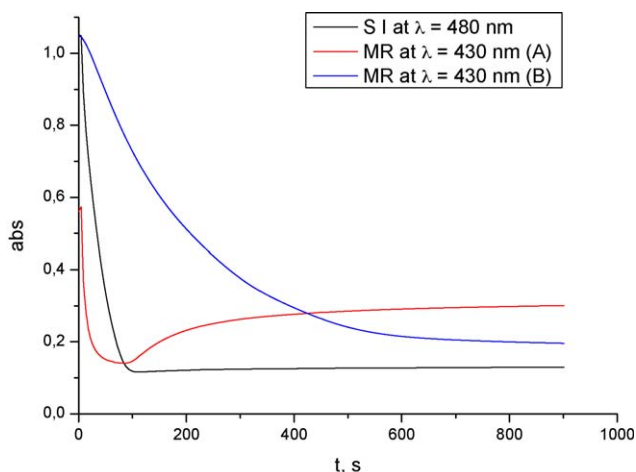

Fig. 3. UV–Vis spectra recorded during the Mn^{2+} catalyzed oxidative degradation of MO by H$_2$O$_2$, when the catalyst was added along with H$_2$O$_2$ to the dye containing buffer solution (A) and when the catalyst was allowed to stand for a longer time in a dye containing buffer solution before addition of H$_2$O$_2$ (B). Reaction conditions: 2×10^{-5} M Mn^{2+}, 5×10^{-5} M AY, 0.01 M H$_2$O$_2$ at pH 8.5 (0.4 M HCO$_3^-$) and 25 °C.

Fig. 4. Comparison of the absorbance *versus* time traces at characteristic wavelengths for the 2×10^{-5} M Mn^{2+} catalyzed oxidative degradation of 5×10^{-5} M dye by 0.01 M H_2O_2 at pH 8.5 (0.4 M HCO_3^-) and 25 °C. The catalytic degradation of MR was performed following two different reaction procedures: (A) the catalyst was added concomitantly with the appropriate amount of H_2O_2 and (B) the catalyst was kept for 20 h [17] in a dye containing bicarbonate solution at pH 8.5, respectively.

oxidative decomposition of 5×10^{-5} M S I and MR by 0.01 M H_2O_2, a rapid catalyst formation followed by a fast oxidation of the substrate at pH 8.5 (0.4 M HCO_3^-) and 25 °C was observed. The time course of the intensity of the characteristic absorption bands for the selected dyes is illustrated in Fig. 4.

For the attempted oxidations of S I and MR a rapid degradation of the dye molecule was observed when the catalyst and H_2O_2 were added simultaneously to the dye containing bicarbonate solution. It was found that the simple Mn^{2+} catalyzed oxidative decomposition of aromatic azo dyes with a functional group adjacent to the azo linkage was significantly accelerated under the same catalytic conditions, which suggests that the presence of electron rich functional groups in the composition of the substrate plays an important role in the formation and stabilisation of the reactive Mn^{2+} intermediates.

Preliminary results involving Orange II, an *ortho*-hydroxy aromatic dye, revealed that no deactivation as well as no precipitate formation occurs even in the presence of high oxidant concentrations in high bicarbonate containing buffer solutions at longer reactions time (over several days) [10]. The Mn^{2+} ion

catalyzed oxidative degradation of MR is a complicated process. The UV–Vis spectra recorded during these reactions in the presence of MR, when appropriate amount of catalyst and H_2O_2 were added simultaneously to the dye containing solution (Fig. 5A), and when the catalyst was let to stand for 20 h in a dye and bicarbonate containing solution (B), revealed a complicated oxidation process.

Upon initiation of the reaction by simultaneous addition of the catalyst and H_2O_2 to the dye containing buffer solution (Fig. 5A) or by addition of H_2O_2 to a pre-activated catalyst and dye containing solution (Fig. 5B), the absorption intensity at $\lambda_{max} = 430$ nm decreased and in both cases shifted to shorter wavelengths. When the reaction was performed in the presence of Mn^{2+} added concomitantly with H_2O_2 to the reaction mixture, a fast decomposition of MR occurred in the first 100 s followed by a second reaction, resulting finally in the increase in absorbance at 430 nm (see Fig. 5A). The second reaction in this case is believed to involve the condensation of the formed intermediates, since Mn^{2+} ions are known to be able to catalyze the condensation of unsaturated organic substrates [19]. Therefore, the pre-catalyst and the dye containing buffer solution were kept for 20 h at room temperature before H_2O_2 addition to the reaction mixture (see Fig. 5B), when a deeply coloured Mn–dye intermediate formed. Furthermore, when the reaction was started by addition of H_2O_2, the oxidative degradation of MR took significantly longer to reach completion. The isosbestic points at 290 nm indicate the formation and subsequent decay of at least one intermediate in the oxidative degradation of MR (see Fig. 5B).

3.1.3. Phenolic derivatives and flavonoid dyes (M, PNP and TA)

In separate experiments, the oxidative degradation of phenolic derivatives and flavonoidic dyes were studied under the same experimental conditions. The dyes M, PNP and TA were oxidized under the above mentioned experimental conditions (see Fig. 6).

The experimental results showed that the presence of hydroxy groups in the composition of the dye accelerates the formation of the stabilized Mn–dye reactive intermediates, and upon addition of H_2O_2 a fast and efficient decomposition of the studied substrates occurred within less than 200 s. A reasonable reaction rate was also obtained for the oxidative degradation of TA, a high molecular weight polyphenolic derivative, widely distributed throughout the plant world. When TA was oxidized, it was observed that the catalytic reaction is over in about 100 s, although for an efficient
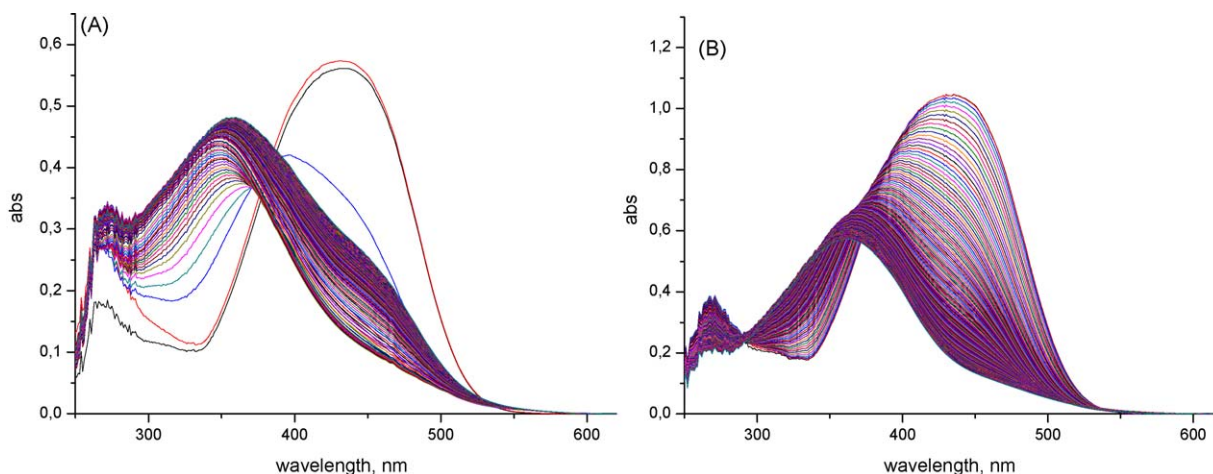

Fig. 5. UV–Vis spectra recorded during the Mn^{2+} catalyzed oxidative degradation of MR by H_2O_2, when the catalyst was added simultaneously with H_2O_2 to the dye containing buffer solution (A) and when the catalyst was allowed to stand for 20 h in a dye containing buffer solution (B). The reaction conditions were: 2×10^{-5} M Mn^{2+}, 5×10^{-5} M MR, 0.01 M H_2O_2 at pH 8.5 (0.4 M HCO_3^-) and 25 °C.
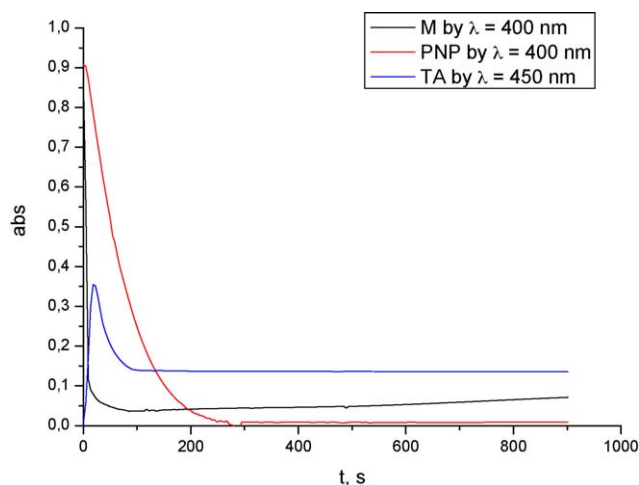
Fig. 6. Comparison of the absorbance *versus* time traces at different wavelengths corresponding to the maximum absorbance of M and PNP at 400 nm and of TA at 450 nm for the 2×10^{-5} M Mn^{2+} catalyzed oxidative degradation of 5×10^{-5} M dye by 0.01 M H$_2$O$_2$ at pH 8.5 (0.4 M HCO$_3^-$) and 25 °C.

oxidative decomposition of the dye higher amounts of oxidizing agent are required (see Fig. S4, Supporting Information).

3.1.4. Complex-formation between Mn^{II} and organic dyes

In order to understand the unusual high activity of simple Mn^{II} ions in the oxidative degradation of different highly stable organic dyes, it is essential to examine potential reaction pathways and relevant equilibria. Initial studies on the complex-formation starting from a Mn^{II} containing aqueous solution in the presence of Orange II revealed that a six-membered ring chelate complex with a stoichiometry of 1:1 is formed under catalytically relevant experimental conditions [10]. Similarly, experiments carried out in the presence of other organic dyes, *viz.* PADA, PNP and MO, revealed coordination of the dye to the Mn^{II} centre. Changes in the UV–Vis spectrum of 5×10^{-5} M Mn^{II} in a 0.1 M HCO$_3^-$ containing solution at ambient temperature upon titration with dye evidenced the formation of a 1:1 Mn^{II}–dye complex in the case of selected dyes. In this study, the value of K_{eq} was determined through a constant variation of the Mn^{2+} and dye concentrations, respectively. Independent measurements were repeated between five and eight times, and the reported data are the mean values of at least five determinations. In the case of PADA, selected data are shown in Fig. 7, where the solid line represents a fit of Eq. (1) to the data

$$
\text{dye} + \text{Mn}^{2+} \overset{K_{eq}}{\rightleftharpoons} (\text{Mn}^{II} - \text{dye})
$$
$$
A_x - A_0 = (A_\infty - A_0)K_{eq}[\text{PADA}]/(1 + K_{eq}[\text{PADA}]) \quad (1)
$$
$$
\Delta\text{Abs} = \Delta\text{Abs}_\infty \times K_{eq}[\text{PADA}]/(1 + K_{eq}[\text{PADA}])
$$

The values of A_0 and A_∞ in Eq. (1) represent the absorbance of PADA and of the in situ build PADA$\cdots$Mn^{II} complex, respectively, and A_x is the absorbance at any Mn^{II} concentration. The value of K_{eq} was calculated from Eq. (1) to be $(4.2 \pm 0.6) \times 10^4$ M^{-1}, indicating a relatively weak coordination of the dye to the metal centre. A likely coordination mode of the dye to the Mn^{II} centre is presented in Fig. 8.

Moreover, in the case of PNP, an example of a dye coordinating to the metal centre in a monodentate mode, it was also possible to observe specific spectroscopic changes that indicated the coordination of the dye molecule to the fully aquated Mn^{II} ion. However, in the case of MO, an azo dye which contains no *ortho* substituents and has a very low affinity for metal binding, no significant spectral changes were observed upon addition of a 5×10^{-5} M Mn^{II} to a 5×10^{-5} M MO aqueous solution (for experimental data see Figs. S5 and S6, Supporting Information).
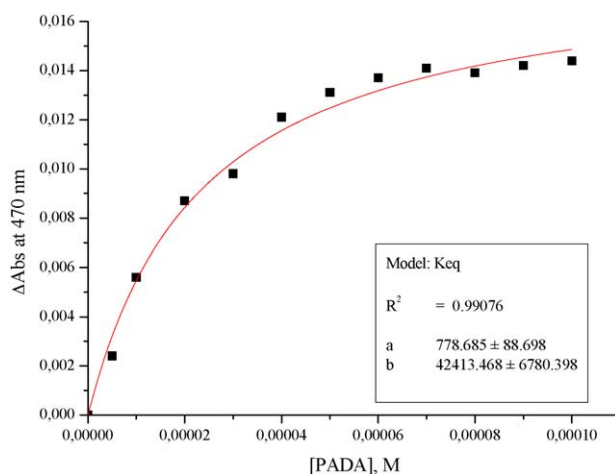

Fig. 7. Change in absorbance at 460 nm on addition of different concentrations of PADA to 5×10^{-5} M Mn^{II} in aqueous carbonate solution (0.1 M HCO$_3^-$) at pH 8.5 and 22 °C.

3.1.5. DFT calculations

Before studying the interaction mechanism of suitable Mn–dye derivatives, the geometries and relative energies of several complexes were investigated using DFT calculations. To gain deeper insight into the coordination mode of the Mn^{II} centre and the stabilisation ability of the studied dyes in aqueous solution, DFT (B3LYP(CPCM: H$_2$O)/(LANL2DZp//B3LYP/LANL2DZp+ZPE(B3LYP/ LANL2DZp) calculations were performed for a series of seven different Mn^{II}–dye complexes. A comparison of the calculated complexation energies relative to [Mn(H$_2$O)$_6$]$^{2+}$ are given in Fig. 9.

The observed trend in Fig. 9 can be attributed to the preferentially improved stabilisation of the reactive Mn^{2+} centre by electron donating OH groups present in S I, PNP and M, in comparison with the electron donating ability of the pyridine nitrogen in PADA, which is in good agreement with the experimental results. In addition to the usual stabilisation by the chelate-effect, further stabilisation by dπ–π^* back-donation of the azo group in S I leads to the formation of an -3.4 kcal mol^{-1} more favourable complex in an octahedral environment. In the presence of MR, a less energetically favoured intermediate is formed due to weak coordination of the electron rich manganese centre to the electron-withdrawing carboxyl group. Furthermore, the coordination in an unusual seven-membered chelate ring, adopting non-planar, distorted trigonal bipyramidal geometry was calculated to be an energetically highly unfavourable (22.1 kcal mol^{-1}) conformer. In order to compare the relative complex-formation energies with the stabilisation energy of the postulated manganese catalysts, further DFT calculations on the well characterized manganese 2,2′:6′,2″ terpyridine complex (Mn^{II}(- TERPY)) was performed. In earlier work, it was shown that the catalytic activity of the complex is greatly enhanced by the presence of π-electron donors, *i.e.* hydroxyl group, compared to the unsubstituted terpyridine complex [20]. Given the ability to chelate with the nitrogen atoms of all pyridine rings, one can assume a meridional coordination mode of terpyridine with Mn^{2+} resulting in
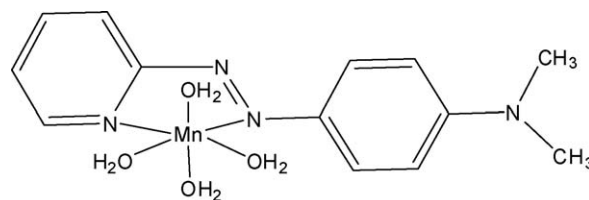

Fig. 8. Proposed structure for a 1:1 Mn^{2+}–PADA complex formed in aqueous solution under the selected experimental conditions.
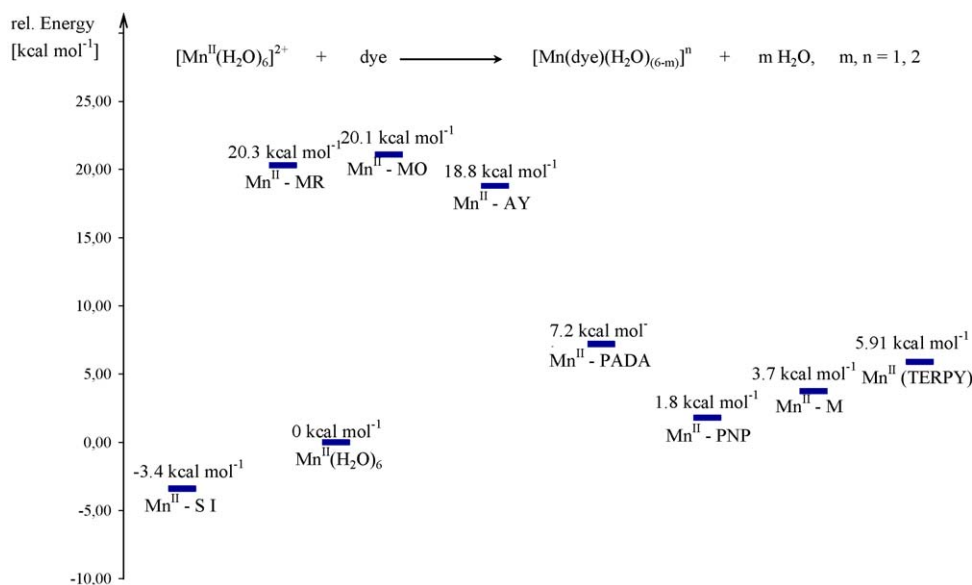
Fig. 9. Relative complexation energies (B3LYP(CPCM:H₂O)/(LANL2DZp//B3LYP/LANL2DZp+ZPE(B3LYP/LANL2DZp)) for the selected Mn^{II}–dye intermediates.

an energetically favoured complex (see Fig. S7, Supporting Information). The calculated relative complexation energy for Mn^{II}(TERPY) is 5.9 kcal mol^{-1}. Contrary to our expectations, the formed intermediate is 9.3 kcal mol^{-1} less stable than the in situ formed Mn^{II}–S I complex.

For comparison, further calculated structures of expected intermediates formed in the presence of the studied dyes are shown in Figs. S8A–E, Supporting Information.

3.2. Optimization of the reaction conditions for the catalytic oxidation reactions

3.2.1. pH effect

Apart from the fact that the oxidative degradation of the studied organic dyes occurred efficiently, the optimization of the process by analyzing the effect of several parameters such as pH, H₂O₂ and Mn^{2+} concentration, was investigated in more detail.

The kinetics of the manganese catalyzed oxidative degradation of the selected dyes was studied in 0.4 M NaHCO₃ buffer solution in the pH range from 8.0 to 9.5 at 25 °C. The decomposition of the dyes was followed by monitoring the absorbance change at the characteristic λ_{max} of each dye. Experimentally determined observed first order rate constants for the Mn^{II} catalyzed oxidative degradation of all the examined dyes by H₂O₂ were found to pass through a maximum on changing the solution pH as shown in Fig. 10 for PADA, MO and PNP.

For all systems the rate of oxidation increases with increasing pH and goes through a maximum, which is found at a pH between 8.2 and 8.5, suggesting that the same reactive manganese species and the same in situ formed oxidizing agent is responsible for the decomposition of the various substrates. The increase in the reaction rate over the above mentioned pH range is attributed to the formation of HCO₄$^-$, a versatile oxidizing agent formed in aqueous bicarbonate solution according to Eq. (2) [21]

$$HCO_3^- + H_2O_2 \overset{K=0.32\pm0.02M^{-1}}{\rightleftharpoons} HCO_4^- + H_2O \qquad (2)$$
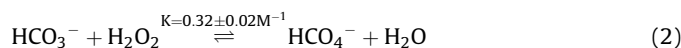
In control experiments, by performing the oxidation reactions in the presence of peroxycarbonate instead of H₂O₂ in 0.4 M bicarbonate containing buffer solution at pH 8.5, no difference in the reactivity was observed (see Fig. S9, Supporting Information). The decrease in oxidation rate at higher pH is partly due to the

subsequent formation of Mn(OH)₂ precipitates at higher pH and to the deprotonation of HCO₃$^-$ that becomes significant at pH above 8–9 [22]. This results in a decrease in the HCO₃$^-$ concentration in equilibrium (2), which reduces the concentration of peroxycarbonate present in solution.

3.2.2. Critical role of bicarbonate

Previous results [10], as well as the results described above, establish that the bicarbonate concentration plays an important role in the overall oxidation reaction. The Mn^{II} catalyzed oxidative degradation of selected dyes by using H₂O₂ as an oxidizing agent could be significantly enhanced in all cases through increasing the total carbonate concentration in the reaction mixture. This can be accounted for in terms of the equilibrium formulated in Eq. (2). The total carbonate concentration was varied between 0.05 and 0.5 M. The dependence of the observed first-order rate constants on the total bicarbonate concentration is shown in Fig. 11.

In the present case, the catalytic reaction leads to a second order dependence of k_{obs} on the HCO₃$^-$ concentration with a third order rate constant of 0.43 ± 0.02 M^{-2} s^{-1} for PADA, 0.30 ± 0.01 M^{-2} s^{-1} for MO and 0.160 ± 0.004 M^{-2} s^{-1} for PNP, suggesting that two
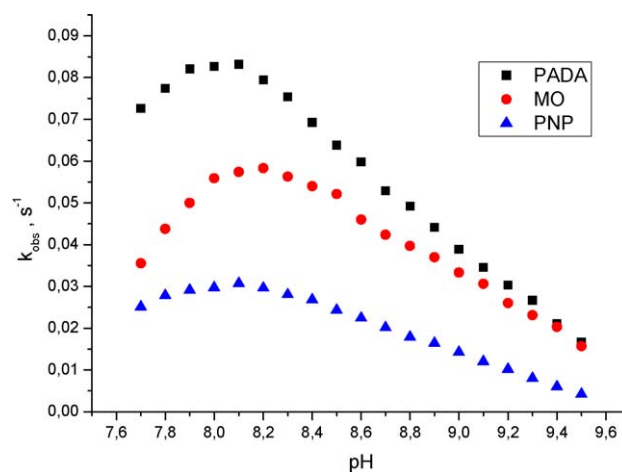

Fig. 10. pH dependence of the 2×10^{-5} M Mn^{II} catalyzed oxidative degradation of 5×10^{-5} M dye by 0.01 M H₂O₂ in 0.4 M bicarbonate buffer solution at ambient temperature.
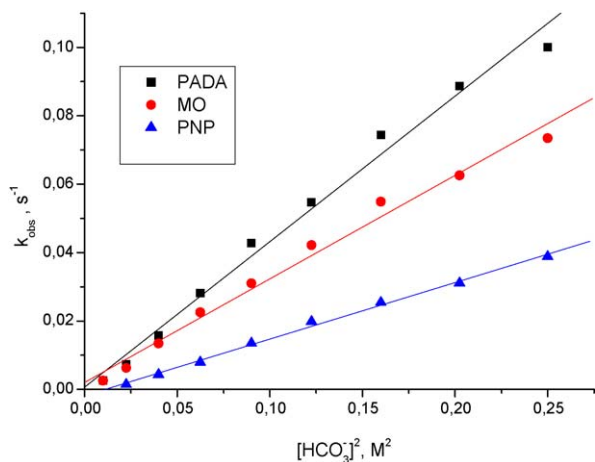
Fig. 11. Second-order bicarbonate concentration dependence of k_{obs}. Experimental conditions: 2×10^{-5} M Mn(NO$_3$)$_2$, 5×10^{-5} M dye, 0.01 M H$_2$O$_2$, pH 8.5, 25 °C.

equivalents of HCO$_3^-$ are involved in the oxidation mechanism. Consistent with preliminary rate studies on the oxidative degradation of Orange II [10], it was found that one equivalent of HCO$_3^-$ is required for the formation of the more reactive [Mn^{II}(CO$_3$)(H$_2$O)$_4$] intermediate (see further discussion), and the second equivalent of HCO$_3^-$ is required for the in situ formation of peroxycarbonate in (2), known to be a versatile oxidizing agent.

In the view of these findings we decided to study the influence of the H$_2$O$_2$ concentration on the manganese catalyzed oxidation of selected organic dyes by H$_2$O$_2$ under mild reaction conditions.

3.2.3. Effect of H$_2$O$_2$ concentration on the manganese catalyzed oxidative degradation of various dyes

The effect of the H$_2$O$_2$ concentration on the oxidation reaction course of three different dyes (PADA, MO and PNP) was studied in detail by variation of its concentration between 5×10^{-5} and 0.03 M H$_2$O$_2$ in a 0.3 and 0.5 M bicarbonate containing solution at pH 8.5 and ambient temperature. At lower H$_2$O$_2$ concentrations (10^{-3} and 5×10^{-3} M) a fast oxidation reaction occurs in the first few seconds followed by a rapid consumption of H$_2$O$_2$ which finally results in a partial and inefficient decolouring of the dye.

The results presented in Fig. 12 show that the observed rate constant initially increased on increasing the H$_2$O$_2$ concentration in the case of PADA and MO, and reached a limiting value at higher oxidant concentrations (see Fig. 12A and B). However, in the case of PNP a slower but more efficient oxidation of PNP was observed on increasing the H$_2$O$_2$ concentration (see Fig. 12C), which suggests that on starting from hexaaqua Mn^{II} in the presence of structurally different organic dyes, catalyst precursors of different reactivity are formed. Moreover, in the presence of PNP, the partial decomposition of the in situ formed reactive Mn$\cdots$PNP intermediates cannot be completely excluded under the catalytic reaction conditions when larger amounts of H$_2$O$_2$ are added to the solution, since in the presence of PNP mainly non-chelated complexes are formed.
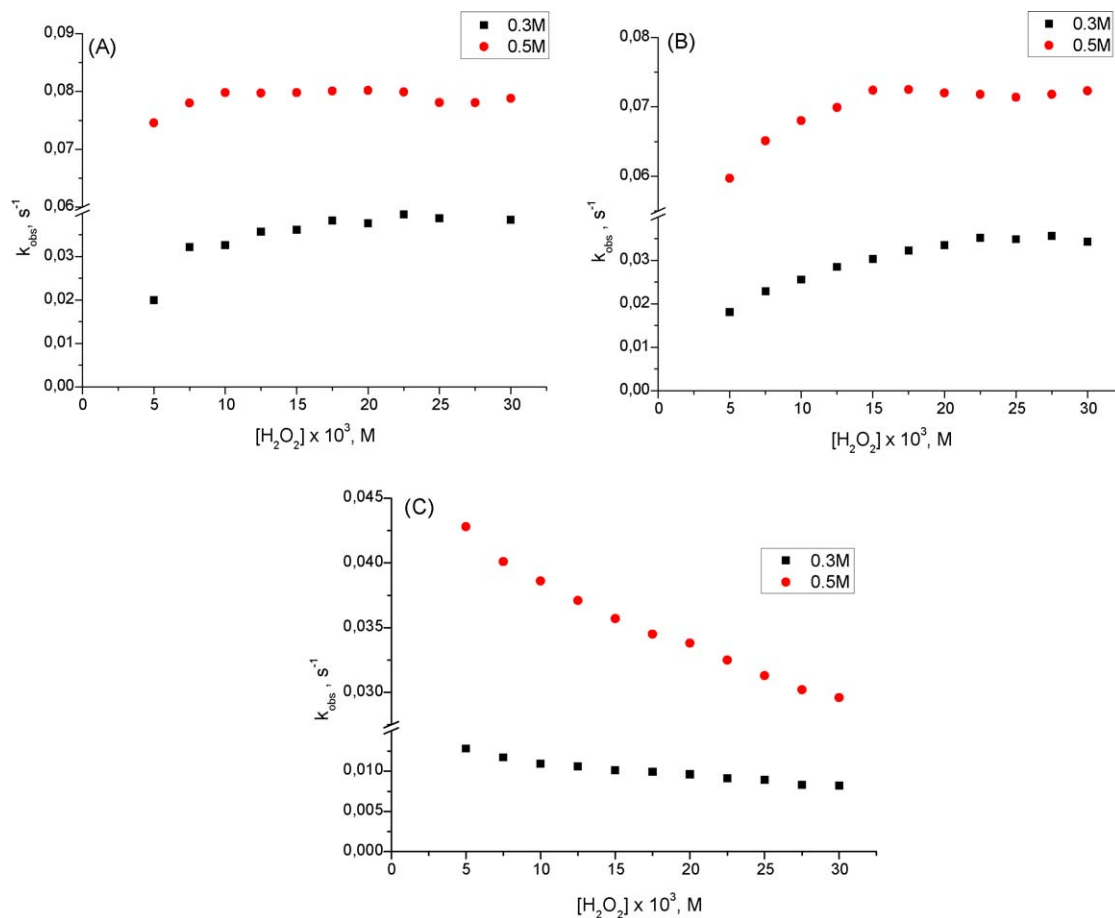

Fig. 12. H$_2$O$_2$ concentration dependence of k_{obs} for the manganese catalyzed oxidative degradation of PADA (A), MO (B) and PNP(C) by H$_2$O$_2$. Reaction conditions: 5×10^{-5} M dye, 2×10^{-5} M Mn(NO$_3$)$_2$, in 0.3 M and 0.5 M containing bicarbonate solution at pH 8.5 and 25 °C.
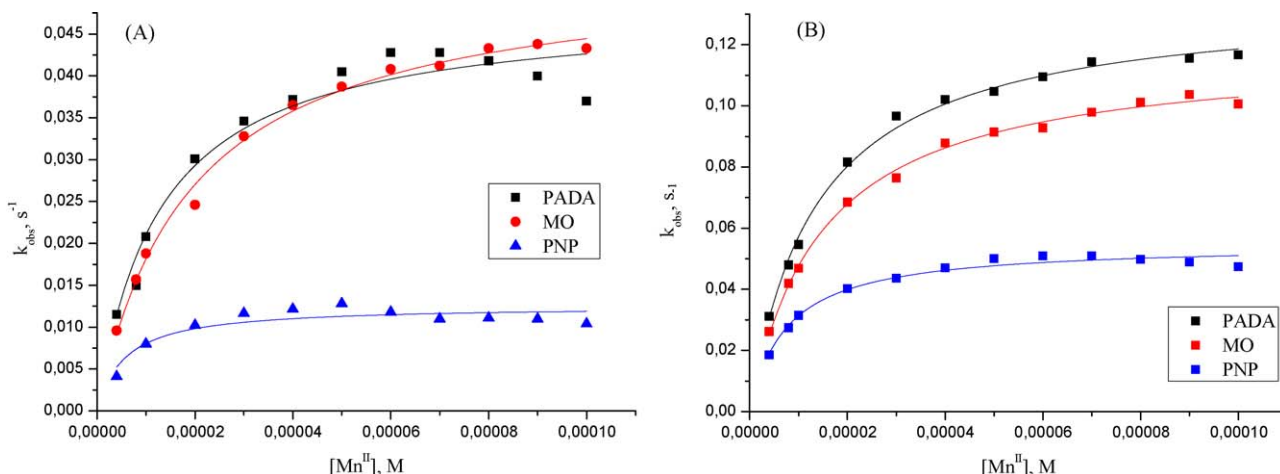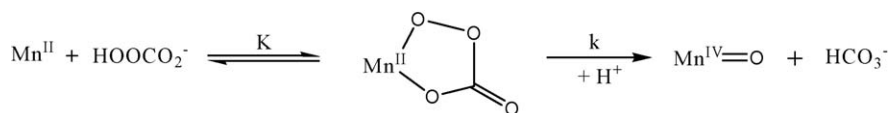
Fig. 13. Mn^{2+} concentration dependence of k_{obs}. Reaction conditions: 5×10^{-5} M dye, 0.01 M H_2O_2 in 0.3 M (A) and 0.5 M (B) containing bicarbonate solution at pH 8.5 and 25 °C.

Scheme 1. Proposed reactions steps for the formation of the catalytically active manganese intermediate in the presence of H_2O_2 in a bicarbonate containing solution.

3.2.4. Effect of the manganese concentration on the oxidative degradation of various dyes by H_2O_2

To evaluate the effect of the catalyst concentration on the oxidative degradation of different organic dyes by H_2O_2, kinetic studies were performed by the simultaneous addition of solutions containing various concentrations of $Mn(NO_3)_2$ along with a 0.01 M solution of H_2O_2 to a 0.05 M solution of the dye in two different bicarbonate containing buffer solutions (0.3 and 0.5 M) at pH 8.5 and 25 °C. Plots of the observed rate constant as a function of $[Mn^{2+}]$ at different carbonate concentrations are presented in Fig. 13.

The experiments performed with different catalyst concentrations show that the oxidation rate constant increased with increasing concentration of the in situ formed catalyst and reached a maximum value at high catalyst concentration for all the selected dyes (see Fig. 13A and B). The observed rate profile can be accounted in terms of the general reaction mechanism proposed in Scheme 1.

The rate law for the proposed mechanism in Scheme 1 is given by Eq. (3). The calculated values of k and K obtained from the non-linear concentration dependences in Fig. 13 are summarized in Table 2

$$k_{obs} = \frac{kK[Mn(II)]}{1 + K[Mn(II)]} \qquad (3)$$

3.2.5. EPR studies on the in situ formed intermediates

In order to gain more information on the nature of the catalytically active high valent $Mn^{IV}{=}O$ intermediate formed in the

Table 2
Values of k and K for the $Mn(NO_3)_2$ catalyzed oxidation of PADA, MO and PNP by H_2O_2 at pH 8.5 and 25 °C.

Dye	0.3 M HCO_3		0.5 M HCO_3	
	k (s^{-1})	K ($\times 10^{-3}$, M^{-1})	k (s^{-1})	K ($\times 10^{-3}$, M^{-1})
PADA	0.05 ± 0.02	78 ± 13	0.130 ± 0.002	74 ± 4
MO	0.05 ± 0.01	52.1 ± 0.3	0.120 ± 0.001	67 ± 3
PNP	0.012 ± 0.001	179 ± 53	0.050 ± 0.001	133 ± 13

presence of H_2O_2 in a bicarbonate containing buffer solution, low-temperature EPR measurements were performed under catalytically relevant conditions at 7 K. The initial Mn^{II} containing aqueous solution gave a six-line pattern centred at $g \approx 2$ which are split by isotropic hyperfine coupling with the ^{55}Mn nucleus ($I = 5/2$) (see Fig. S10, Supporting Information). Each of the six hyperfine lines consists of five overlapping, electron spin transitions within the $S = 5/2$ electron spin multiplet of Mn^{2+}. Complex-formation with bicarbonate further reduces the symmetry of the ligand field around the Mn^{2+} ion and thereby causes the zero-field splitting to increase. Larger zero-field splitting in the complex results in broader electron spin transitions and thus weaker intensity of the six-line EPR signal compared to the more symmetric Mn_{aq}^{2+} ion (see Fig. S11, Supporting Information). By addition of H_2O_2 to the Mn^{2+} containing bicarbonate solution, a new broad signal of low intensity at $g \approx 4$ was observed, which was not present in the original spectrum of the Mn^{II}-bicarbonate containing buffer solution (see Fig. 14). EPR signals at $g \approx 4$ are characteristic for high-spin Mn^{IV} ($S = 3/2$) species in an octahedral environment having $D < h\nu$, which also have a higher amplitude feature at $g \approx 2$ [8,23,24].

Of significant importance in the present case are the strong EPR spectral features exhibited by the in situ generated $Mn^{IV}{=}O$ intermediate in the $g \approx 2$ region with only minor components at $g \approx 4$, which differs from other reported $Mn^{IV}{=}O$ intermediates [8]. The EPR spectra of d^3 Mn^{IV} ions in an axial field ($E/D = 0$) are often difficult to interpret as they greatly depend on the magnitude of the zero-field splitting parameters [25]. When the value for the axial zero-field splitting parameter D is large, a strong signal is found at low field along with a weaker $g \approx 2$ component. Such is the case for Mn^{IV} complexes with hard oxygen-rich catecholate [26] and sorbitalate [27] ligands. In another case, where D is small, the $g \approx 2$ signal dominates with relatively weak low field signals. This is seen for example for sulfur-containing thiohydroxamate [25b] and dithiocarbamate [28] manganese(IV) complexes.

In an attempt to find evidence for the formation of Mn^{III} as the catalytic species responsible for the catalytic oxidation of different organic dyes and to proof that the reaction follows a radicalic oxidation reaction, EPR measurements were performed in the
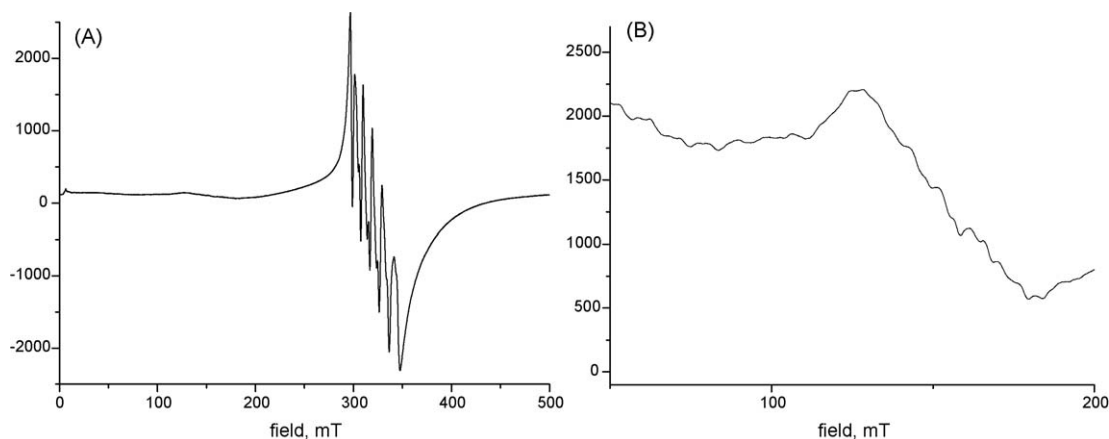
Fig. 14. EPR spectra of a Mn^{II} containing buffer solution after addition of H_2O_2 at pH 8.5 recorded over the entire spectral range (A) and in a range from 0 mT to 200 mT (B), respectively. Experimental conditions: 10^{-4} M $Mn(NO_3)_2$, 0.02 M H_2O_2 in 0.4 M HCO_3^- at pH 8.5 and 7 K. EPR: 9.4 GHz, 7 K, 2 mW microwave power.

presence of different radical scavenger, i.e. ^tBuOH and ABTS, in aqueous solution. EPR and UV–Vis data showed no evidence for Mn^{III} species or for radical formation. In all the studied cases, the addition of a radical scavenger in the reaction mixture had no influence on the oxidation reaction course (see Fig. S12, Supporting Information), providing further evidence that Mn^{IV} predominates as catalytic species in the reaction.

In order to clarify the mechanism of the catalytic reaction further, UV–Vis spectroscopic measurements on the in situ formation of the high-valent Mn-oxo intermediate were performed under the above mentioned experimental reaction conditions (see Fig. S13, Supporting Information). After addition of H_2O_2 to a Mn^{II} containing buffer solution, the solution colour changed to deep yellow and a characteristic broad band for Mn^{IV}=O with a maximum at 460 nm was formed. The presence of Mn^{IV}=O suggests a two-electron oxidation of Mn^{2+} to a high-valent Mn^{IV}=O species as a potential oxidation catalyst in this reaction. Similar spectroscopic observations for the formation of high-valent Mn^{IV}=O intermediates were reported by Sureshan and Bhattacharya [29] and DeVos and Bein [30] in the case of olefin epoxidation catalyzed by different manganese complexes.

3.3. Stability of the in situ formed Mn^{II}–dye precursors

The stability and re-usability of the catalyst are important parameters for the efficiency of catalytic reactions. Manganese salts in aqueous solution are able to form very reactive aquated intermediates which in the absence of any further stabilizing ligands lead to the formation of catalytically inactive Mn complexes. Depending on the HCO_3^- concentration in the reaction mixture, $Mn^{II}\cdots HCO_3^-$ complexes of different stoichiometry can be formed in solution. $Mn^{II}\cdots HCO_3^-$ intermediates are relatively stable and an irreversible deactivation of the catalyst occurs within less than 20 min. On the other hand, no precipitate formation as well as no deactivation of the catalytically active manganese intermediate could be observed in the presence of a coordinating organic substrate, i.e. organic dye, over a long period of time (1–4 days) in a high bicarbonate concentration (0.4 M) containing buffer solution under catalytically relevant experimental conditions. Representative experimental data for the catalytic reaction performed in the presence of PADA- and MR-stabilized Mn^{2+} intermediates and H_2O_2 in bicarbonate containing buffer solution at ambient temperature are shown in Fig. S14A and B (Supporting Information), respectively. Representative data for the catalytic reaction performed in the presence of PNP-stabilized Mn^{2+} intermediate are illustrated in Fig. 15A and B.

As seen in Fig. 15A and B, a successful stabilisation of the in situ formed reactive Mn^{2+} intermediate could be achieved in the presence of structurally different organic substrates in bicarbonate containing aqueous solution at pH 8.5. Noteworthy is that an efficient stabilisation of reactive Mn^{2+} intermediates could be
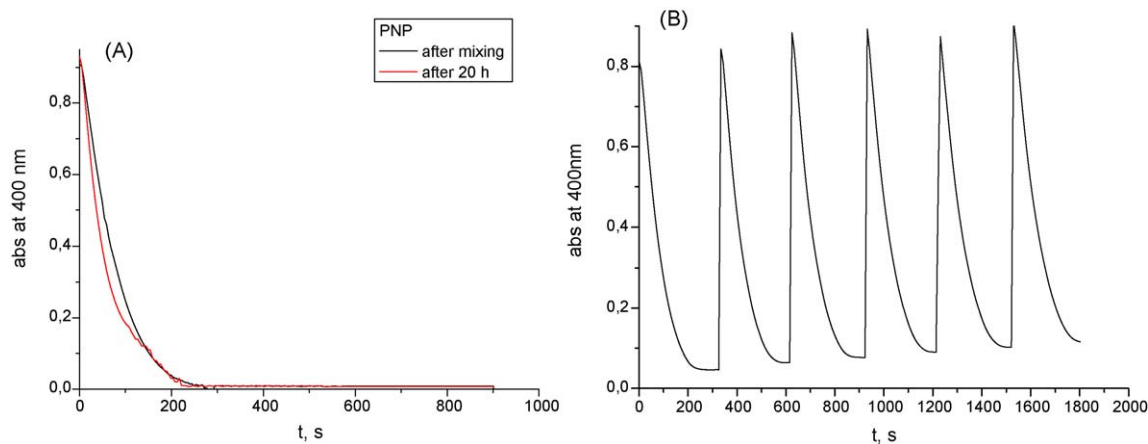

Fig. 15. (A) Absorbance changes observed at 400 nm for the 2×10^{-5} M $Mn(NO_3)_2$ catalyzed oxidative degradation of 5×10^{-5} M PNP by 0.01 M H_2O_2 immediately after mixing (−), and after addition of 0.01 M H_2O_2 to a 20 h old reaction mixture at pH 8.5 (0.4 M HCO_3^-) and 25 °C (−). (B) Spectral changes observed at 400 nm for the repeated addition of 5×10^{-5} M PNP and 0.01 M H_2O_2 to a 20 h old catalyst containing reaction mixture under the same experimental conditions as mentioned in A.
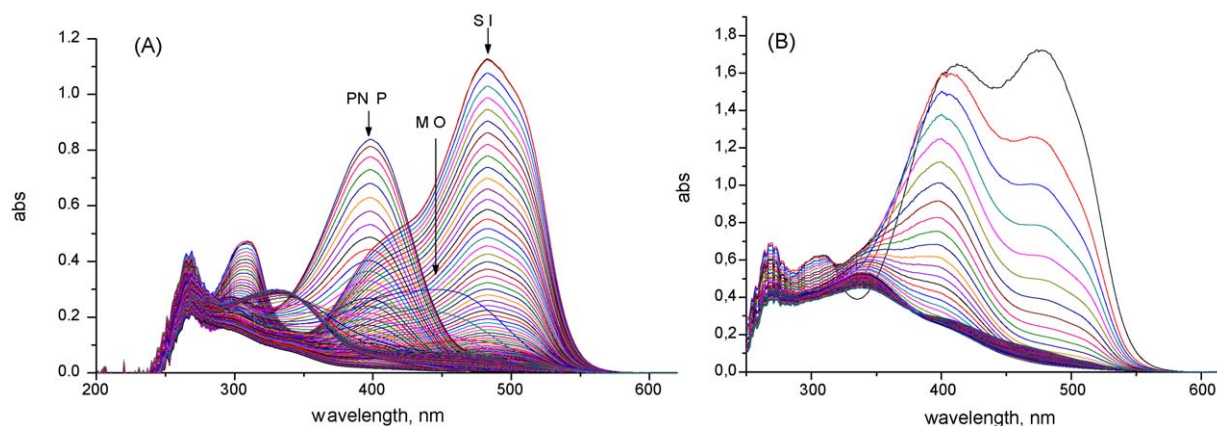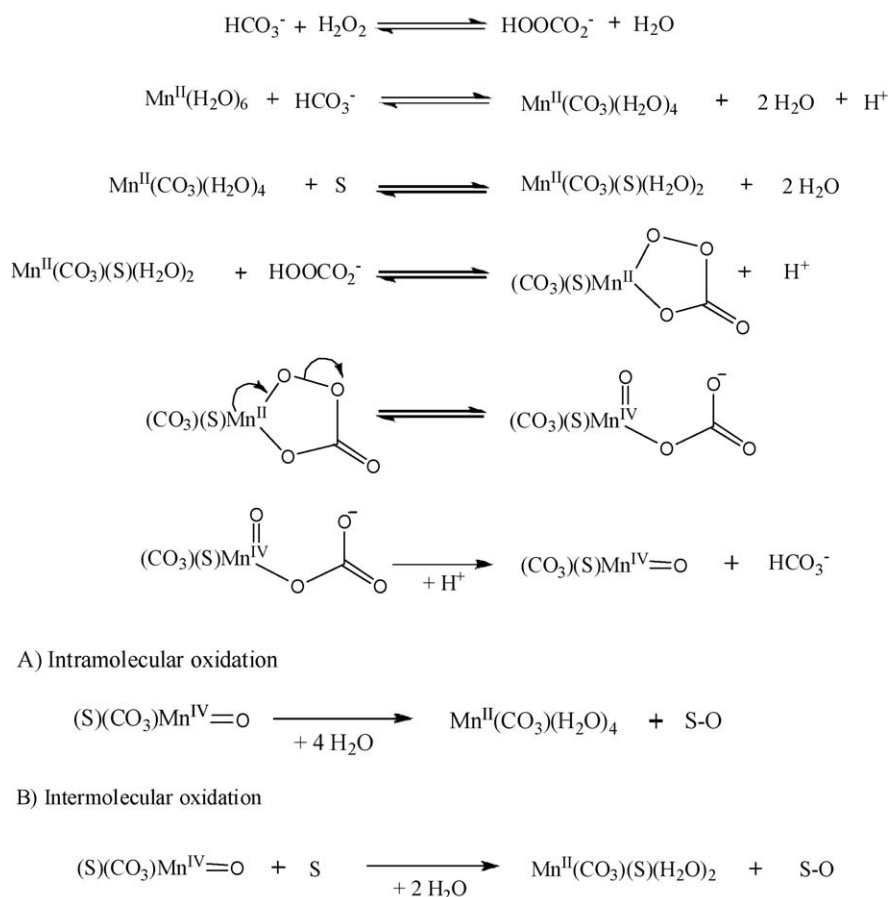
Fig. 16. Oxidative degradation of 5×10^{-5} M organic dyes (S I, MO and PNP) in the presence of 2×10^{-5} M Mn^{II}, 0.01 M H_2O_2 at pH 8.5 (0.4 M HCO_3^-) and ambient temperature, when the selected dyes were successively added along with fresh amounts of 0.01 M H_2O_2 to the reaction mixture (A), and all the dyes and the appropriate amount of 0.03 M H_2O_2 were added simultaneously to the bicarbonate containing solution (B).

achieved even in the presence of an organic dye with low binding affinity or binding in a monodentate manner. In all cases, the catalytic cycle could be repeated several times without any significant loss of activity during the oxidation reaction, indicating an excellent stability of the in situ formed catalyst. The experimental results illustrated in Fig. 15B for PNP provide clear evidence for the high efficiency of the in situ formed catalyst in the presence of monodentate coordinating dyes under the above mentioned experimental reaction conditions.

3.4. Practical application of the process

The possible practical application of the Mn^{II} catalyzed oxidative degradation of organic dyes by H_2O_2 in bicarbonate containing solution under mild reaction conditions, was studied for the case where more than one dye of different structures were present in the reaction mixture (see Fig. 16).

The data in Fig. 16 indicate that the oxidation of highly stable dyes, viz. S I, MO and PNP, can effectively be catalyzed by simple

Scheme 2. Proposed reaction mechanism for the Mn(II) catalyzed oxidative degradation of organic dyes (S) by H_2O_2 in a bicarbonate containing aqueous solution under mild reaction conditions, when the product formation involves either an intramolecular (A) or intermolecular (B) oxygen transfer step.

Mn^{II} ions in a bicarbonate containing solution under mild reaction conditions. Upon addition of Mn^{II} to a bicarbonate dye containing solution, a stable Mn^{II}–dye intermediate is formed. The results in Fig. 16A indicate that in the presence of S I a stable manganese intermediate is formed, which after addition of H_2O_2 and in situ formation of $Mn^{IV}=O$, efficiently catalyzes the oxidative decomposition of further substrates such as MO and PNP. Similarly, a mixture of all three dyes was successfully oxidized using the same catalytic system (see Fig. 16B), which clearly indicates the practical applicability and high efficiency of this rather simple catalytic system.

3.5. Mechanistic interpretation

Taking into account all obtained spectroscopic and kinetic data, reaction Scheme 2 can be proposed for the Mn^{2+} catalyzed oxidative degradation of various dyes (S) by H_2O_2 in carbonate solution under catalytically relevant experimental conditions.

The proposed reaction mechanism involves in the first step the in situ formation of peroxycarbonate, a versatile oxidizing agent in a pH range from 8 to 9. This reaction step is also considered to be the rate-limiting step in the proposed mechanism. Furthermore, the experimental results presented above in-line with previous studies [8,10,31], evidenced that bicarbonate has an important role in the in situ formation of reactive Mn(II)-bicarbonate intermediates under experimental conditions, since the positively charged Mn_{aq}^{2+} complex is actually not able to catalyze H_2O_2 disproportionation. Depending on the bicarbonate concentration in the reaction mixture, different bicarbonate containing Mn^{2+} intermediate is formed. In earlier works [32] it was evidenced that the first bicarbonate coordinates to Mn^{2+} in a bidentate mode and $[Mn^{2+}(HCO_3)(H_2O)_4]^+$ is formed. Under our experimental conditions (pH 8.5) it is suggested that the in situ formed bicarbonate complex deprotonates to form $[Mn^{2+}(CO_3)(H_2O)_4]$ ($pK_a \sim 8.5$ [32] for the bicarbonate bound to Mn^{2+}). At higher bicarbonate concentrations, other bicarbonate containing complexes of different stoichiometry can be formed. Unfortunately, these in situ generated bicarbonate complexes are not stable at ambient temperature and precipitate as catalytically inactive $MnCO_3$.

In this study, an efficient stabilisation of the $[Mn^{2+}(CO_3)(H_2O)_4]$ intermediate could be reached in the presence of an electron rich organic molecule, such as the substrate itself. Our experimental results revealed that in the presence of a dye, highly stable $[Mn^{2+}(CO_3)(S)(H_2O)_2]$ (S = organic dyes) complexes are formed. We propose that in the subsequent step, nucleophilic attack of in situ formed peroxycarbonate on the dye stabilized, reactive $Mn^{II}(CO_3)(S)(H_2O)_2$ centre, produces a quasi-stable Mn^{II}-η^2-peroxycarbonate complex, which undergoes heterolytic cleavage of the peroxide bond to form the high-valent $Mn^{IV}=O$ intermediate. This intermediate can now in an intramolecular or intermolecular manner transfer an oxygen atom to the substrate molecule as shown in Scheme 2.

The formation of small molecular non-toxic oxidation products is believed to involve an intra- or intermolecular oxygen transfer step as shown in Scheme 2 followed by the regeneration of the active catalyst.

4. Conclusions

The present study provides a viable solution for the efficient and clean oxidative degradation of highly stable organic dyes and sheds light on the stabilisation of in situ formed highly reactive manganese intermediates.

The reported experimental data along with the performed DFT calculations revealed that starting from a simple Mn^{II} salt in aqueous solution, highly reactive intermediates are formed, which in the absence of any further coordinating ligand, rapidly decompose to catalytically inactive $MnCO_3$, $Mn(OH)_2$ or MnO_2. A successful stabilisation of the in situ formed catalytically active intermediate was achieved through the σ,π-coordination of the selected organic dye. In all cases, the formation of highly efficient and reusable catalyst for the oxidative decomposition of different stable organic dyes by H_2O_2 under mild reaction conditions was observed.

The kinetic studies performed as a function of pH provides relevant information concerning the nature of the oxidizing agent involved in the reaction. It was found that the pH is a critical issue for the rate of the oxidation process due to its influence on the deprotonation of the bicarbonate ions, the formation of peroxycarbonate in solution, and the deprotonation of aquated Mn^{2+}. Moreover, the oxidative degradation of the selected organic dyes is catalytic only in carbonate containing aqueous solution. Consistent with preliminary rate studies on the oxidative degradation of Orange II, the catalytic reaction leads to a second order dependence of k_{obs} on the HCO_3^- concentration. It was found that one equivalent of HCO_3^- is required for the formation of the more reactive $[Mn^{II}(H_2O)_4(CO_3)]$ intermediate, and the second equivalent is required for the in situ formation of peroxycarbonate, known to be a versatile oxidizing agent.

Kinetic studies suggest the formation of high valent $Mn^{IV}=O$ species as key catalytic intermediate on addition of H_2O_2 to a Mn^{II} containing carbonate buffer solution under mild reaction conditions. EPR spectra of the catalytically active intermediate in frozen solution at 7 K showed a weak signal at $g \approx 4$ and a strong sextet at $g \approx 2$, consistent with Mn^{IV} in an octahedral environment.

The experimental results clearly demonstrate the considerable potential of this system for clean and efficient oxidation of organic substrates in aqueous solution at ambient temperature.

Appendix A. Supplementary data

Supplementary data associated with this article can be found, in the online version, at doi:10.1016/j.apcatb.2009.12.013.

References

[1] (a) P.A. Frey, A.D. Hegeman (Eds.), Enzymatic Reaction Mechanisms, Oxford University Press, New York, 2007, pp. 465–480;
(b) Special topic issue, Chem. Rev. 96 (1996) 2237–3042;
(c) B. Meunier (Ed.), Biomimetic Oxidations Catalyzed by Transition Metal Complexes, Imperial College Press, London, 2000, pp. 269–307;
(d) H. Sigel, A. Siegel (Eds.), Electron Transfer Reactions in Metalloproteins. Metal Ions in Biological Systems, vol. 27, M. Dekker, New York, 1991, pp. 75–91.
[2] B.S. Lane, K. Burgess, Chem. Rev. 103 (2003) 2457–2474.
[3] M. Palucki, N.S. Finney, P.J. Pospisil, M.L. Güler, T. Ishida, E.N. Jacobsen, J. Am. Chem. Soc. 120 (1998) 948–954.
[4] E. Rose, B. Andrioletti, S. Zrig, M. Quelquejeu-Etheve, Chem. Soc. Rev. 34 (2005) 573–583.
[5] (a) K. Wieghardt, W. Schmidt, B. Nuber, J. Weiss, Chem. Ber. 112 (1979) 2220–2230;
(b) K.E. Sibbons, K. Shastri, M. Watkinson, Dalton Trans. (2006) 645–661;
(c) B.C. Gilbert, J.R. Lindsay Smith, M.S. Newton, J. Oakes, R.P. iParts, Org. Biomol. Chem. 1 (2003) 1568–1577.
[6] J.W. De Boer, W.R. Browne, J. Brinksma, P.L. Alsters, R. Hage, B.L. Feringa, Inorg. Chem. 46 (2007) 6353–6372.
[7] J. Oakes, P. Gratton, I. Weil, J. Chem. Soc., Dalton Trans. (1997) 3805–3809.
[8] B.S. Lane, M. Vogt, V.J. DeRose, K. Burgess, J. Am. Chem. Soc. 124 (2002) 11946–11954.

[9] K.-P. Ho, W.-L. Wong, K.-M. Lam, C.-P. Lai, T.H. Chan, K.-Y. Wong, Chem. Eur. J. 14 (2008) 7988–7996.

[10] E. Ember, S. Rothbart, R. Puchta, R. van Eldik, New J. Chem. 33 (2009) 34–49.

[11] (a) A.D. Becke, J. Phys. Chem. 97 (1993) 5648–5652;
(b) C. Lee, W. Yang, R.G. Parr, Phys. Rev. B 37 (1988) 785–789;
(c) P.J. Stephens, F.J. Devlin, C.F. Chabalowski, M.J. Frisch, J. Phys. Chem. 98 (1994) 11623–11627;
(d) P.J. Hay, W.R. Wadt, J. Chem. Phys. 82 (1985) 270–283;
(e) P.J. Hay, W.R. Wadt, J. Chem. Phys. 82 (1985) 284–298;
(f) P.J. Hay, W.R. Wadt, J. Chem. Phys. 82 (1985) 299–310;
(g) S. Huzinaga (Ed.), Gaussian Basis Sets for Molecular Calculations, Elsevier, Amsterdam, 1984.

[12] M.J. Frisch, G.W. Trucks, H.B. Schlegel, G.E. Scuseria, M.A. Robb, J.R. Cheeseman, J.A. Montgomery, Jr., T. Vreven, K.N. Kudin, J.C. Burant, J.M. Millam, S.S. Iyengar, J. Tomasi, V. Barone, B. Mennucci, M. Cossi, G. Scalmani, N. Rega, G.A. Petersson, H. Nakatsuji, M. Hada, M. Ehara, K. Toyota, R. Fukuda, J. Hasegawa, M. Ishida, T. Nakajima, Y. Honda, O. Kitao, H. Nakai, M. Klene, X. Li, J.E. Knox, H.P. Hratchian, J.B. Cross, C. Adamo, J. Jaramillo, R. Gomperts, R.E. Stratmann, O. Yazyev, A.J. Austin, R. Cammi, C. Pomelli, J.W. Ochterski, P.Y. Ayala, K. Morokuma, G.A. Voth, P. Salvador, J.J. Dannenberg, V.G. Zakrzewski, S. Dapprich, A.D. Daniels, M.C. Strain, O. Farkas, D.K. Malick, A.D. Rabuck, K. Raghavachari, J.B. Foresman, J.V. Ortiz, Q. Cui, A.G. Baboul, S. Clifford, J. Cioslowski, B.B. Stefanov, G. Liu, A. Liashenko, P. Piskorz, I. Komaromi, R.L. Martin, D.J. Fox, T. Keith, M.A. Al-Laham, C.Y. Peng, A. Nanayak-kara, M. Challacombe, P.M.W. Gill, B. Johnson, W. Chen, M.W. Wong, C. Gonzalez, J.A. Pople, Gaussian, Inc., Wallingford CT (2004).

[13] (a) R. Puchta, R. Meier, N.J.R. van Eikema Hommes, R. van Eldik, Eur. J. Inorg. Chem. (2006) 4063–4067;
(b) A. Scheurer, H. Maid, F. Hampel, R.W. Saalfrank, L. Toupet, P. Mosset, R. Puchta, N.J.R. van Eikema Hommes, Eur. J. Org. Chem. (2005) 2566–2574;
(c) P. Illner, A. Zahl, R. Puchta, N.J.R. van Eikema Hommes, P. Wasserscheid, R. van Eldik, J. Organomet. Chem. 690 (2005) 3567–3576;
(d) Ch.F. Weber, R. Puchta, N.J.R. van Eikema Hommes, P. Wasserscheid, R. van Eldik, Angew. Chem. 117 (2005) 6187–6192;
(e) Ch.F. Weber, R. Puchta, N.J.R. van Eikema Hommes, P. Wasserscheid, R. van Eldik, Angew. Chem Int. Ed. 44 (2005) 6033–6038;
(f) M. Alzoubi Basam, F. Vidali, R. Puchta, C. Dücker-Benfer, A. Felluga, L. Randaccio, G. Tauzher, R. van Eldik, Dalton Trans. (2009) 2392–2399.

[14] (a) V. Barone, M. Cossi, J. Phys. Chem. A 102 (1998) 1995–2001;
(b) M. Cossi, N. Rega, G. Scalmani, V. Barone, J. Comp. Chem. 24 (2003) 669–681.

[15] Y. Peng, D. Fu, R. Liu, F. Zhang, X. Xue, Q. Xu, X. Liang, Appl. Catal. B: Environ. 79 (2007) 163–170.

[16] (a) P.J. Krueger, in: S. Patai (Ed.), The Chemistry of the Hydrazo, Azo and Azoxy Groups, Wiley, New York, 1975, p. 168, Part 1;
(b) H.A. Gazzaz, B.H. Robinson, Langmuir 16 (2000) 8685–8691;
(c) R.W. Sabnis, Handbook of Acid–Base Indicators, CRC Press (Taylor and Francis Group), London, 2008;
(d) L. Pentimalli, Tetrahedron 5 (1959) 27–37;
(e) A. Siegel, H. Siegel, Metal Ions in Biological Systems, vol. 37, Marcel Dekker, New York, 1999, 330;
(f) S.V. Jovanovic, S. Steenken, M. Tosic, B. Marjanovic, M.G. Simic, J. Am. Chem. Soc. 116 (1994) 4846–4851;
(g) S.K. Dentel, J.Y. Bottero, K. Khatib, H. Demougeot, J.P. Duguet, C. Anselme, Water Res. 29 (1995) 1273–1280.

[17] Even if the complexation of the fully aquated Mn^{II} ions in the presence of a selected dye is complete within a few minutes, in order to study the stability of the in situ formed complex, the pre-catalyst containing solution was stored for a longer period of time at ambient temperature (between 15 min and 20 h).

[18] (a) D. Moussa, A. Doubla, K.Y. Georges, J.L. Brisset, IEEE Trans. Plasma Sci. 35 (2007) 444–453;
(b) J. Gong, J. Wang, W. Xie, W. Cai, J. Appl. Electrochem. 38 (2008) 1749–1755.

[19] Z. Szeverenyi, L. Simandi, J. Mol. Catal. 51 (1989) 155–201.

[20] T. Wieprecht, J. Xia, U. Heinz, J. Dannacher, G. Schlingloff, J. Mol. Catal. A: Chem. 203 (2003) 113–128.

[21] D.E. Richardson, H. Yao, K.M. Frank, D.A. Bennett, J. Am. Chem. Soc. 122 (2000) 1729–1739.

[22] J.R. Lindsay Smith, B.C. Gilbert, A.M. Payeras, J. Murray, T.R. Lowdon, J. Oakes, R.P.I. Prats, P.H. Walton, J. Mol. Catal. A: Chem. 251 (2006) 114–122.

[23] S.M. Saadeh, M.S. Lah, V.L. Pecoraro, Inorg. Chem. 30 (1991) 8–15.

[24] R.P. John, A. Sreekanth, M.R. Prathapachandra Kurup, H.-K. Fun, Polyhedron 24 (2005) 601–610.

[25] (a) E. Pedersen, H. Toftlund, Inorg. Chem. 13 (1974) 1603–1612;
(b) S. Pal, P. Ghosh, A. Chakravorty, Inorg. Chem. 24 (1985) 3704–3706;
(c) J.C. Hempel, L.O. Morgan, W.B. Lewis, Inorg. Chem. 9 (1970) 2064–2072.

[26] K.D. Magers, G.C. Smith, D.T. Sawyer, Inorg. Chem. 19 (1980) 492–496.

[27] D.T. Richens, D.T. Sawyer, J. Am. Chem. Soc. 101 (1979) 3681–3683.

[28] K.L. Brown, R.M. Golding, P.C. Healy, K.J. Jessop, W.C. Tennant, Aust. J. Chem. 27 (1974) 2075–2081.

[29] C.A. Sureshan, P.K. Bhattacharya, J. Mol. Catal. A: Chem. 130 (1998) 73–78.

[30] D.E. DeVos, T. Bein, J. Organomet. Chem. 520 (1996) 195–200.

[31] M.B. Yim, B.S. Berlett, P.B. Chock, E.R. Stadtman, Proc. Natl. Acad. Sci. 87 (1990) 394–398.

[32] J. Dasgupta, A.M. Tyryshkin, Y.N. Kozlov, V.V. Klimov, G.C. Dismukes, J. Phys. Chem. B 110 (2006) 5099–5111.